Mar Geophys Res (2006) 27:253–266
DOI 10.1007/s11001-006-9006-1

ORIGINAL PAPER

Crustal analysis of the Ulleung Basin in the East Sea (Japan Sea) from enhanced gravity mapping

Chan Hong Park · Jeong Woo Kim · Nobuhiro Isezaki · Daniel R. Roman · Ralph R. B. von Frese

Received: 8 September 2005 / Accepted: 28 July 2006 / Published online: 21 October 2006

Abstract To facilitate geological analyses of the Ulleung Basin in the East Sea (Japan Sea) between Korea and Japan, shipborne and satellite altimetry-derived gravity data are combined to derive a regionally coherent anomaly field. The 2-min gridded satellite altimetry-based gravity predicted by Sandwell and Smith [Sandwell DT, Smith WHF (1997) J Geophys Res 102(B5):10,039–10,054] are used for making cross-over adjustments that reduce the errors between track segments and at the cross-over points of shipborne gravity profiles. Relative to the regionally more homogeneous satellite gravity anomalies, the longer wavelength components of the shipborne anomalies are significantly improved with minimal distortion of their shorter wavelength components. The resulting free-air gravity anomaly map yields a more coherent integration of short and long wavelength anomalies compared to that obtained from either the shipborne or satellite data sets separately. The derived free-air anomalies range over about 140 mGals or more in amplitude and regionally correspond with bathymetric undulations in the Ulleung Basin. The gravity lows and highs along the basin's margin indicate the transition from continental to oceanic crust. However, in the northeastern and central Ulleung Basin, the negative regional correlation between the central gravity high and bathymetric low suggests the presence of shallow denser mantle beneath thinned oceanic crust. A series of gravity highs mark seamounts or volcanic terranes from the Korean Plateau to Oki Island. Gravity modeling suggests underplating by mafic igneous rocks of the northwestern margin of the Ulleung Basin and the transition between continental and oceanic crust. The crust of the central Ulleung Basin is about a 14–15 km thick with a 4–5 km thick sediment cover. It may also include a relatively weakly developed buried fossil spreading ridge with approximately 2 km of relief.

Keywords Shipborne and satellite gravity · Cross-over adjustment · Ulleung Basin · Gravity modeling · Transitional crust · Fossil ridge

C. H. Park
Marine Environment Department, Korea Ocean Research & Development Institute, Ansan 426-744, Korea

J. W. Kim (✉)
Department of Geoinformation Engineering, Sejong University, Seoul 143-747, Korea
e-mail: jwkim@sejong.ac.kr

N. Isezaki
Department of Geology, Chiba University, Chiba 260, Japan

D. R. Roman
National Geodetic Survey, NOAA, Silver Spring, MD 20910, USA

R. R. B. von Frese
Department of Geological Sciences, The Ohio State University, Columbus, OH 43210, USA

Introduction

The crustal properties of the Ulleung Basin (Fig. 1) are important to establish when exploring Korea's offshore energy and mineral resources (Park 1990, 1998), and for improving our understanding of the tectonic development of back-arc basin margins (e.g., Jolivet

Fig. 1 General physiography of the East Sea (Japan Sea) and surrounding regions (after Jolivet and Tamaki 1992). The Ulleung Basin study area is delineated. Annotated features include KYR (Kita-Yamato Ridge); YR (Yamato Ridge); TF (Tsushima Fault); YF (Yangsan Fault); UP (Ulleung Plateau); UIG (Ulleung Interplain Gap)

and Tamaki 1992; Lallemand and Jolivet 1985; Otofuji and Matsushida 1983; Lee et al. 1999). However, within the East Sea/Japan Sea the Ulleung Basin remains poorly understood for its crustal structure and development compared to the better studied Japan and Yamato Basins.

Crustal studies offer contrasting hypotheses regarding the geological properties and evolution of the Ulleung Basin. For example, Tamaki et al. (1990) suggested that oceanic crust flanked by foundered and rifted continental blocks partly floor the mid-Tertiary basins in the East Sea (Japan Sea). Alternatively, Jolivet and Tamaki (1992) proposed that true oceanic crust underlies the Japan Basin and that the Yamato and Ulleung Basins formed on highly extended continental crust intruded by volcanic dikes and sills. However, for the Yamato Basin, Hirata et al. (1989) concluded that the anomalously thick, relatively lower velocity crust is probably oceanic, and comprised extensive volcanic flows and sills. Recent seismic refraction experiments in the Ulleung Basin inferred distinct upper and lower crustal layers with the typical oceanic layer 2 and layer 3 velocities seen in the Yamato Basin, even though the Ulleung Basin includes a much thicker sediment package and a slightly thinner lower crust than the Yamato Basin (Kim et al. 1994; Park et al. 1996). The anomalously thick oceanic crust (>10 km) of the Ulleung Basin probably formed during the earliest stage of seafloor spreading (Lee et al. 1999).

Competing models exist to explain the opening of the East Sea, including the Ulleung Basin. Paleomagnetic studies suggested a fast fan-type opening for the East Sea that resulted from the rotation of southwestern Japan (Kawai et al. 1971; Sasajima 1981; Otofuji and Mastuda 1983; Otofuji et al. 1985; Celaya and McCabe 1987). In contrast, other studies (Lallemand and Jolivet 1985; Jolivet 1986; Kimura and Tamaki 1986) proposed a pull-apart opening guided by a dextral shear zone extending 2,000 km along the eastern margin of the East Sea and the north-south trending Yangsan (YF in Fig. 1) and Tsushima Faults (TF). Jolivet et al. (1995) inferred a complex opening that incorporates the pull-apart opening into the clockwise rotation of SW Japan. However, the lack of extensional deformation along the western margin of the Ulleung Basin does not support this rotational opening (Lee et al. 1999).

Geophysical surveys provide the principal source of geological constraint on the origin of the Ulleung Basin. However, geophysical coverage is largely limited to a number of shipborne gravity surveys and,

most recently, to satellite altimetry-derived gravity data that have disparate anomaly mapping attributes and error sources. Compiling shipborne data from different cruises shows many artificial features that may reflect errors between track segments or at the cross-over points where tracks intersect (Fig. 2). A significant source of these errors probably involves navigation inaccuracies that propagate into the anomaly estimates as erroneous Eötvös effects (e.g., Prince and Forsyth 1988; Torge 1989; Blakely 1995). Additional errors may have resulted from the various surveys using different types of instruments that involve different cross-coupling and off-leveling errors, as well as the use of inconsistent reference fields in reducing the gravity observations. More minor errors from instrumental drift and tare, as well as Earth tide cor-

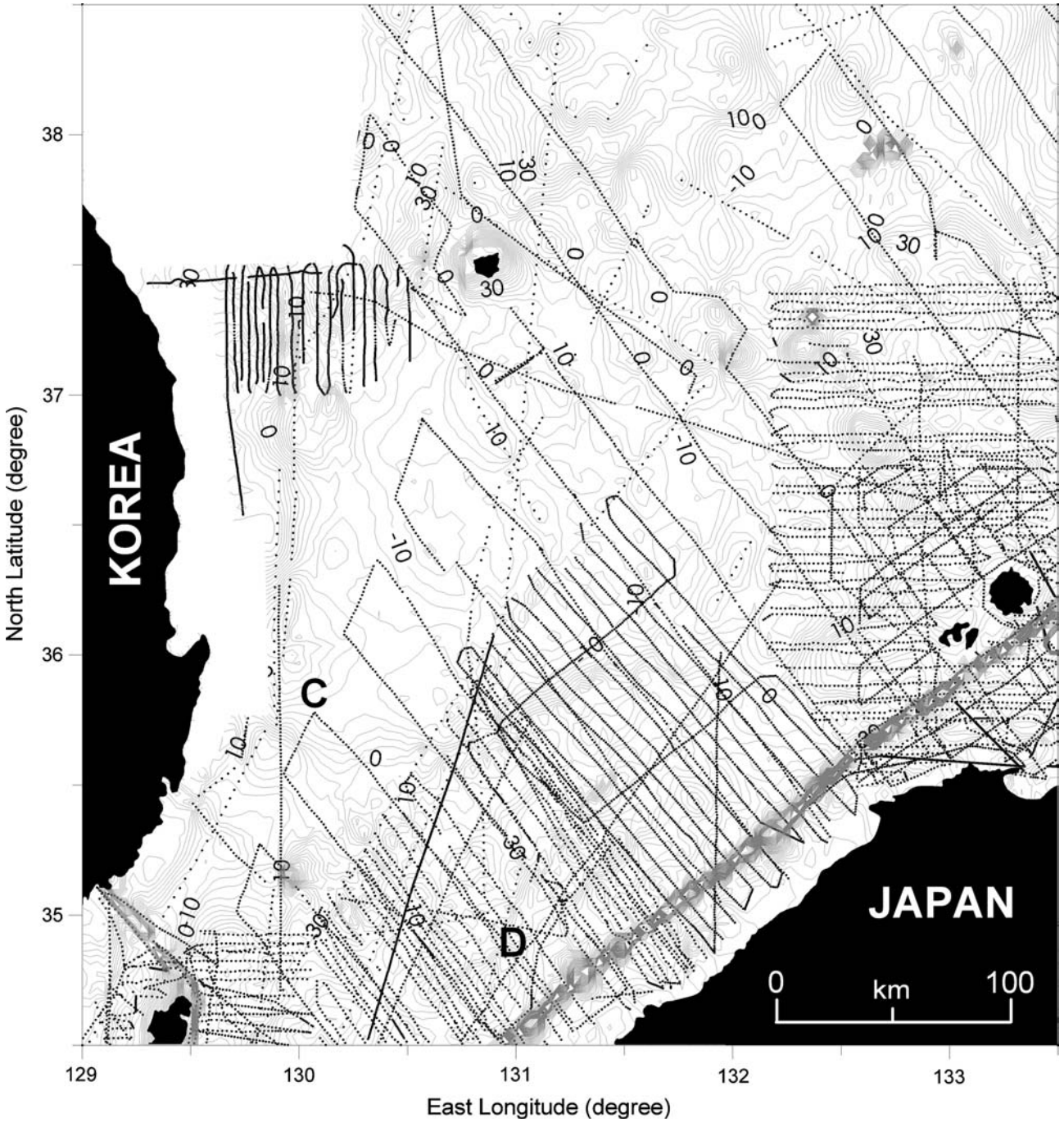

Fig. 2 Shipborne gravity survey track (black dots) coverage and free-air gravity anomalies (mGal) without adjustment for cross-over differences

rections may also be involved. In general, quantifying the accuracy of the shipborne data compilation is very difficult because the individual surveys reflect varying types of navigation, gravity measuring systems, and sea conditions (e.g., Wessel and Watts 1988).

Gravity studies in the East Sea have so far been mostly concentrated in the Yamato Basin or the Japan Basin (e.g., Ishihara 1984; Joshima 1978; Oshida 1992). In general, previous studies of the region including the Ulleung Basin were based on sparsely distributed shipborne or low-resolution satellite gravity data (Suh et al. 1993; Park et al. 1996). However, satellite altimetry-derived gravity data have now become available (Sandwell and Smith 1997) to augment shipborne gravity data where coverage is sparse. Compared to the shipborne data, satellite altimetry-derived gravity data are relatively homogeneous and self-consistent in their regional anomaly properties. However, they are also fundamentally limited in accuracy and resolution of anomaly detail due to limited satellite track coverage and the roughly 7-km footprint of the satellite measurement (Campbell 1995).

In the present study, we combine shipborne and satellite gravity data into a comprehensive gravity anomaly field for the Ulleung Basin. We also assess the quality of the integrated gravity anomaly field and explore it for new details on the poorly known crustal properties and evolution of the Ulleung Basin.

General physiography

The Ulleung Basin ocean floor is fairly smooth in the center and gradually deepens northeastwards from 1,000 m on the basin margin down to about 2,300 m near the Ulleung Interplain Gap (Figs. 1 and 3). The basin is bordered on the west by the steep continental slope of the Korean Peninsula and the Korea Plateau to the north. The seabed morphology of the Ulleung Basin is rough relative to the bathymetry of the other two major sub-basins whose depths exceed 2,200 m. The basin opens northeastwards, and links to the Japan Basin through a narrow and long interplain gap between the Korea Plateau and the Kita-Yamato Ridge (KYR in Fig. 1) and the Yamato Ridge (YR). The channel in the Ulleung Interplain Gap (UIG) runs intermittently along the long axis of the basin connecting the Ulleung Basin to the Japan Basin.

The continental shelf on the east coast of Korea is narrow, with a width of less than 25 km, and grades into a steep slope (Chough 1983). The gentle slope of the Oki Bank borders the basin on the south, whereas the sub-marine extension of the Honshu Shelf borders it to the east. The continental slopes of the eastern Korean Peninsula and the Korea Plateau are steep with large-scale slump pits and scars. Slumps and possible debris flow deposits characterize the base of the slope (Chough et al. 1985). Various scarp features are observed at the foot of the gentle southern slope and the Oki Bank.

Gravity data integration

The crustal study considered the shipborne gravity (Fig. 2), bathymetry (Fig. 3), and satellite altimetry-derived gravity anomalies (Fig. 4) of the area between 34.5–38.5° N and 129.0–133.5° E. The shipborne data included contributions from the global databases of the National Oceanic and Atmospheric Administration's National Geophysical Data Center (NGDC) augmented with additional bathymetry and shipborne gravity data from the Korea Ocean Research and Development Institute (KORDI).

The KORDI gravity data in the Ulleung Basin were acquired in 1993 using a LaCoste-Romberg Model-S shipborne gravimeter aboard the R/V Onnuri. The shipborne gravimeter's measurement accuracy was about 1 mGal after correcting for tides, the ship's movements and other effects. The MDM 300 integrated logging system recorded gravity measurements every minute along with navigation data (e.g., latitude, longitude, and speed). Cruise positions were determined by Global Positioning System (GPS), with survey lines generally running in north–south directions in order to minimize Eötvös effects. The dotted tracks in Fig. 2 show the locations of these shipborne measurements.

At the beginning and end of each cruise, control gravity station measurements were obtained at a port on the southern Korean Peninsula. After converting the measured shipborne gravity data to absolute gravity values, normal corrections using the 1967 Geodetic Reference System and Eötvös corrections were applied. Values with relatively large errors that occurred during or immediately following cruise heading or speed changes were eliminated. The measurements were also corrected for Earth and sea tides. The resultant free-air gravity data were then combined with NGDC shipborne gravity data to obtain the anomaly map shown in Fig. 2.

Significant gaps in data coverage are evident in Fig. 2, especially off the eastern coast of Korea and in the northwest corner of the study region. Data coverage is also quite sparse in the northern third and throughout much of the Ulleung Basin. In addition,

numerous artificial along-track anomaly features indicate severe track-leveling problems caused by uncertainties in navigation, instrument drift, temporal changes in the fields, and other effects. We evaluated the cross-over differences at all 1,530 intersection points of the ship tracks with cubic splines (Wessel and Watts 1988; Wessel 1989). The histogram of the cross-over differences shown in Fig. 5 indicates a mean error of 2.8 mGal with a standard deviation of 16.0 mGal where roughly 33% are greater than 5 mGal.

Inspection of Fig. 2 suggests that the effects of these errors will be quite difficult to sort out on a track-by-track basis. The gaps in data coverage and the

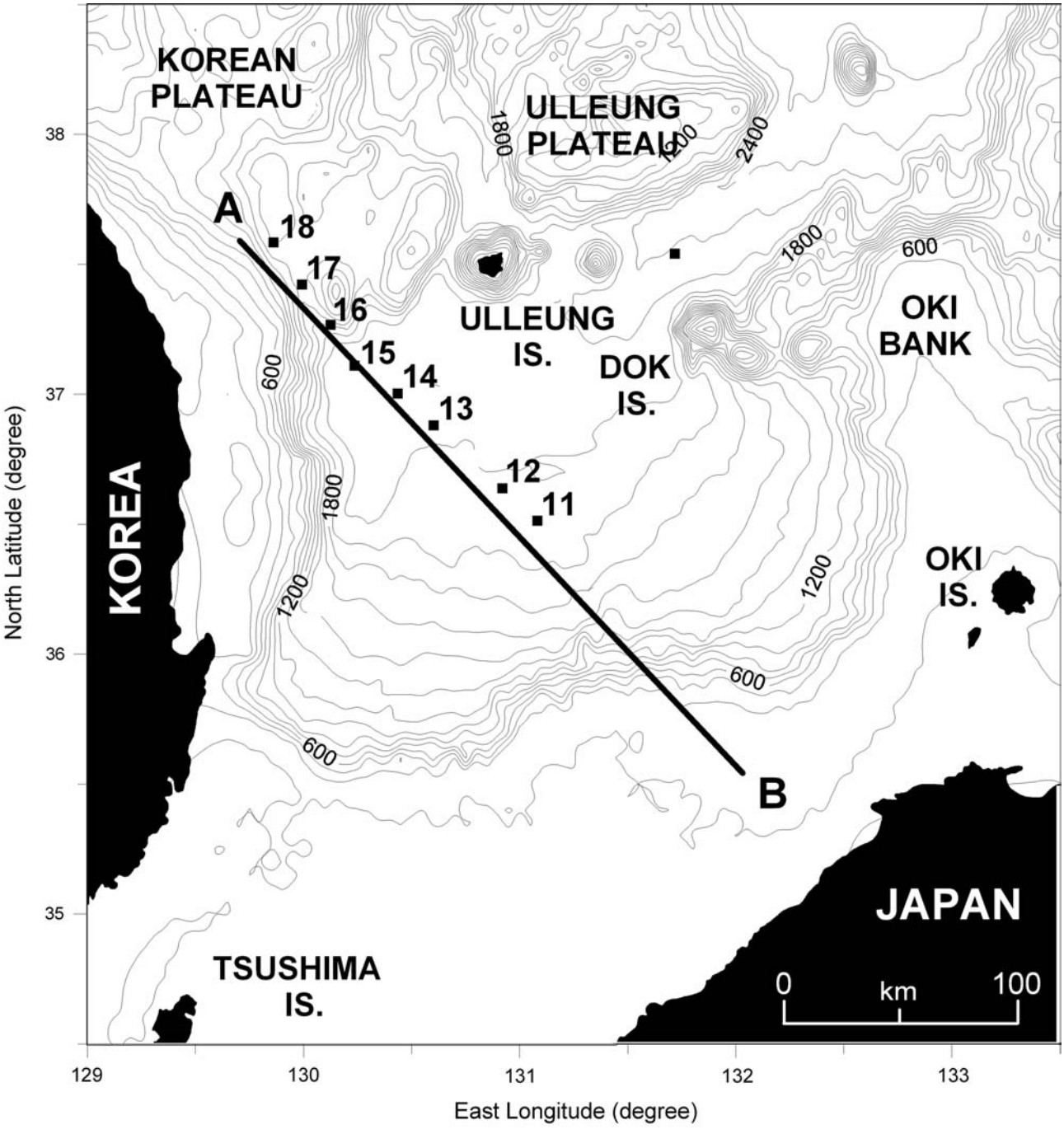

Fig. 3 Bathymetry and geographical features of the Ulleung Basin in the East Sea (Japan Sea). The profile A–B is modeled for its gravity effects in Fig. 12. Numerical identifiers indicate the ocean bottom seismometers (OBS) used to develop the velocity model (Lee et al. 1999) in Fig. 13

leveling disparities between and across tracks also contribute strongly to long-wavelength distortions of the regional anomaly features. However, the satellite altimetry-derived predictions of Sandwell and Smith (1997) shown in Fig. 4 are a supplemental source of coherent regional gravity anomalies that can be used to minimize these effects.

These 2-min free-air anomaly estimates were derived from Geosat GM, Geosat ERM and ERS1 satellite altimetry data. Comparing these anomalies with random shipborne estimates indicates an accuracy of about 4–7 mGal (Sandwell and Smith 1997). The accuracy may improve to perhaps 3 mGal, however, where the ship tracks closely follow Geosat ERM track-lines. The satellite gravity map in Fig. 4 shows relatively smooth and continuous anomaly patterns over the study area that are broadly consistent with the regional features of the shipborne data of Fig. 2.

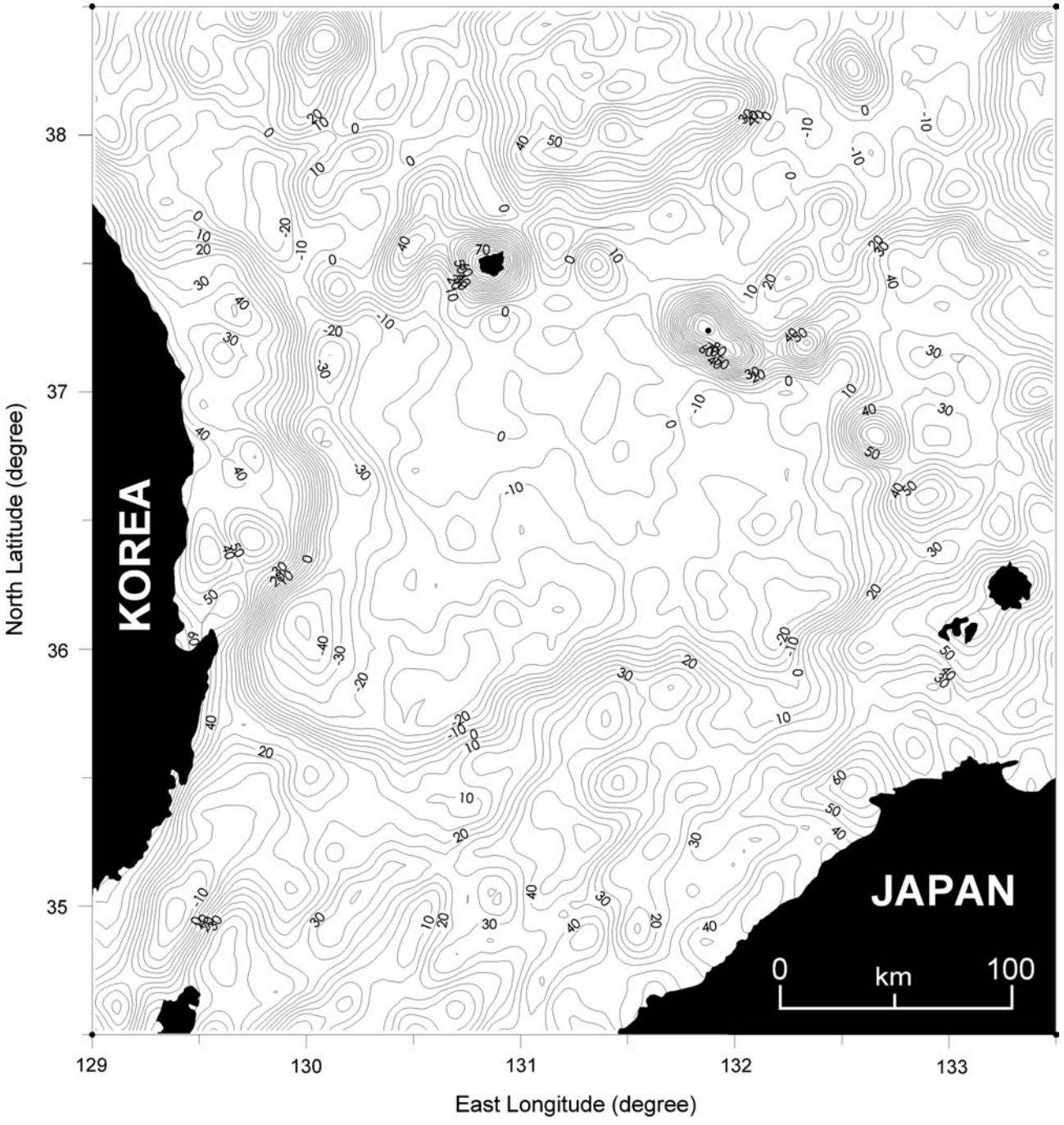

Fig. 4 Satellite altimetry-derived free-air gravity anomalies (mGal) for the Ulleung Basin study area

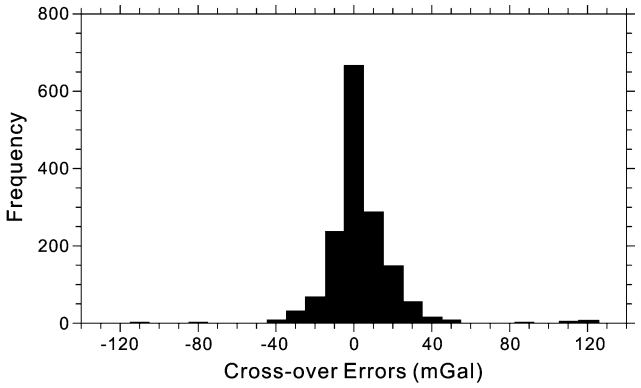

Fig. 5 Histogram of cross-over differences (mGal) in shipborne free-air gravity anomalies

In merging the two data sets, the shipborne gravity data were first sorted into 616 straight-track segments. The satellite data were also regridded onto a 3.4×3.2 km grid using the GMT routines SURFACE and GRIDTRACK (Wessel and Smith 1995). The new grid established points every 2 arc-min along each of the 204 NE-SW profiles with a 5 arc-min interval between profiles. The regridded satellite gravity field matched the original gravity data with negligible error.

Using the cross-over algorithm of Knudsen (1987), all track intersections and their differences were estimated for the segmented shipborne tracks and satellite gravity profiles. A least squares bias adjustment was determined and applied to each track to minimize cross-over differences. Cross-overs were obtained at 5,299 points of intersection where the distance between the profiles was less than 16.75 km. This technique reduced cross-over differences while preserving the relative properties of the gravity anomalies on the individual track segments. Furthermore, the results used cross-over points from all profiles in the study region and thus were more coherent than those based only on the ship-to-ship cross-overs.

Quality assessment of the combined gravity data

To investigate the utility of this new approach, Fig. 6a and b, respectively, show histograms of the gravity differences before and after adjustment of all the ship observation points. The average difference between the shipborne and satellite data was reduced from 5.3 mGal for the uncorrected data to only 0.3 mGal after adjustment. Similarly, the standard deviation of the differences was reduced from 14.5 mGal to 6.1 mGal. The number of cross-over differences greater than 10 mGal was reduced from

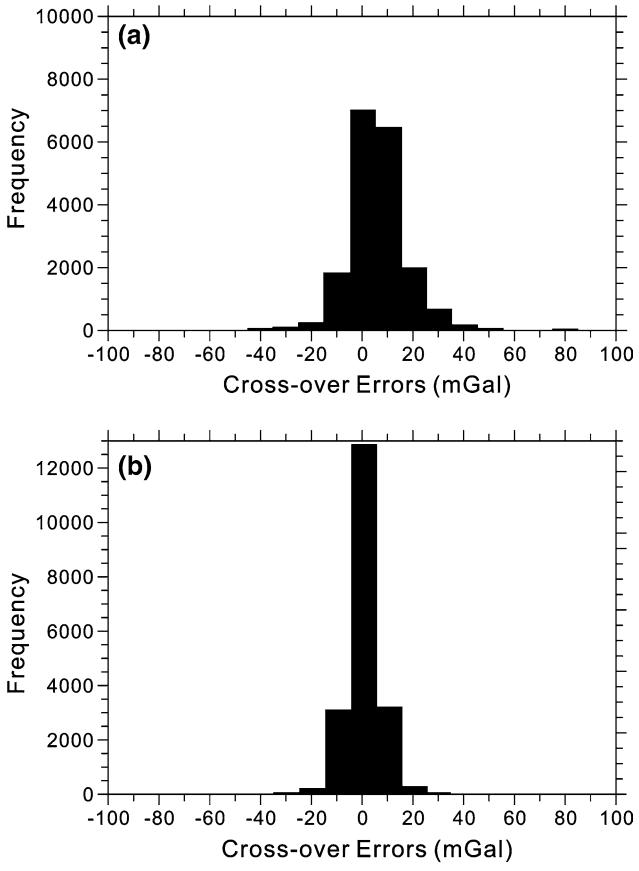

Fig. 6 Histograms of differences (mGal) between the satellite and shipborne gravity data (**a**) before and (**b**) after the cross-over adjustments

64% to 34% after adjustment. The number of differences smaller than 5 mGal increased from 38% to 66%, whereas those less than 10 mGal grew from 63% to 91%. Only 12% of satellite gravity predictions were adjusted by more than 5 mGal, with none exceeding 25 mGal. Additionally, 97% of these differences are concentrated between –5 mGal and –10 mGal. Roughly 33% of the shipborne data were adjusted by more than 5 mGal, whereas less than 11% of the satellite data required an adjustment of this magnitude. In general, the adjusted data sets are now significantly more coherent and permit more robust study of the regional crustal properties of the Ulleung Basin.

The track segment C–D shown in Fig. 7 further demonstrates the effects of these adjustments on the shipborne and satellite gravity data. The adjusted profile closely follows the satellite data track, implying that the adjustments to the shipborne data are relatively greater compared to the satellite data. However, the adjusted data have effectively captured the essential anomaly phase and wavelength properties

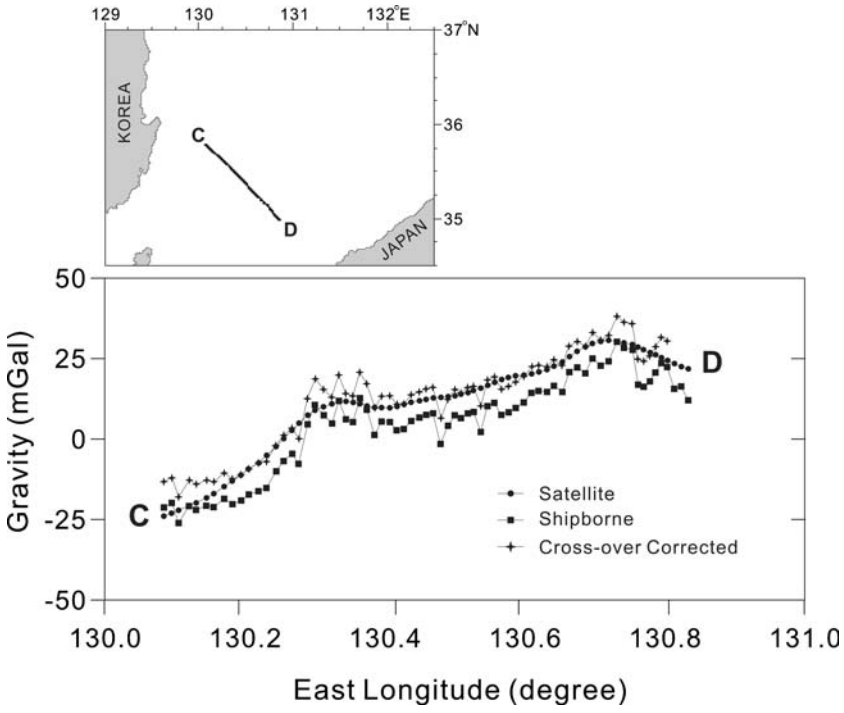

Fig. 7 Satellite and shipborne free-air gravity anomaly profiles demonstrating the effects of the cross-over adjustments along the ship track C–D shown in Fig. 2

of the shipborne and satellite data to an accuracy of about 10 mGal or better.

Figures 8 and 9, respectively, show contour maps of the cross-over adjusted shipborne gravity data and the combined gravity anomalies produced after the cross-over adjustments of the shipborne with the satellite data. In Fig. 10 we show a map in which the satellite altimetry-derived gravity anomalies presented in Fig. 4 were subtracted from the corrected values displayed in Fig. 9 in order to illustrate how the shipborne data augmented the higher frequency properties of the satellite data. These differences indicate generally negative adjustments to the satellite values with magnitudes ranging between –5 mGal and –10 mGal for most regions, but up to more than –15 mGal offshore southwestern Japan.

Geological modeling

The gravity anomalies synthesized in Fig. 9 in combination with available seismic and other geophysical and geological data favor an oceanic rather than a continental crustal type for the basement of the Ulleung Basin. The regional, northeast-trending linear positive anomaly with about 17 mGal of relative amplitude is consistent with higher density crust in the central basin that also may extend between Ulleung and Dok Islands (Kim et al. 1994; Park et al. 1996).

Additional attributes of this dominant positive gravity anomaly are illustrated in Fig. 11, where the free-air gravity anomalies were bandpass filtered for wavelengths between about 10 km and 150 km. Initial studies using available gravity and bathymetric data suggested that the possible source of this feature is the presence of thinned continental crust (Jolivet and Tamaki 1992; Tamaki et al. 1992). However, the analysis of seismic refraction data from ocean bottom seismometer experiments has inferred oceanic crust for the region (Kim et al. 1994). At the basin margin, density transitions from continental to oceanic crust have also been inferred from combined gravity and seismic modeling (Park et al. 1996).

These filtered free-air anomalies reveal a prominent elliptical component extending from the southwest corner of the basin to a circular maximum between Ulleung and Dok Islands. A possible secondary component on the northeastern side of the Ulleung Basin consists of a shorter, roughly sub-parallel elliptical anomaly. In view of the evidence for oceanic crust in the region, these features may mark the raised flanks of an extinct seafloor spreading ridge along which the Ulleung Basin may have opened in a NW–SE direction. The thick dashed line in Fig. 11 marks the possible central graben axis of the spreading ridge.

A quantitative synthesis of the inferred crustal properties for the Ulleung Basin is shown in Fig. 12. Specifically, we used the 2.75-D modeling capablilities of GMSys to model the gravity effects along the NW–SE oriented transect A–B that roughly bisects the inferred fossil ridge. We also used the velocity model

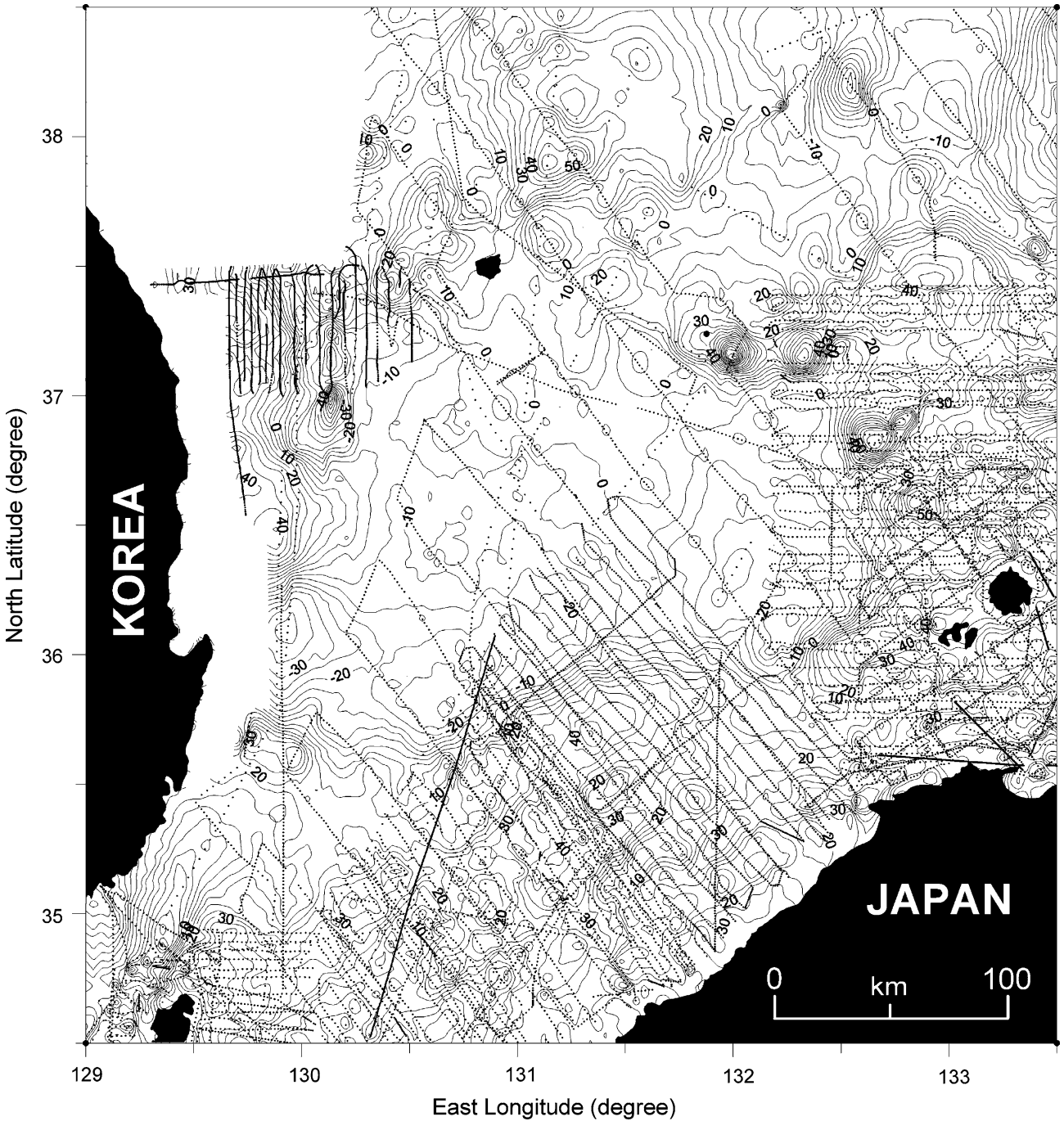

Fig. 8 Map showing the shipborne free-air gravity anomalies (mGal) in the Ulleung Basin region after application of cross-over adjustments

shown in Fig. 13 from Lee et al. (1999) to help constrain crustal boundaries for the gravity modeling.

The modeled mass variations of Fig. 12 include sea water of density 1.030 kg/m^3 and an upper crustal sedimentary package of density 2,300 kg/m^3. The igneous basement rocks of the oceanic upper crust were modeled with density 2,900 kg/m^3, while the flanking felsic continental basement blocks were represented with densities of 2,650–2,850 kg/m^3. Up to 2 km of relief near the center of the oceanic basement block marks the inferred fossil ridge. The presence of mafic igneous rocks underplated to the base of the rifted margin crust was modeled using the density of 3,000 kg/m^3 (Lister et al. 1991) across the transition between oceanic and continental crustal blocks that were inferred from the seismic data. As shown in the

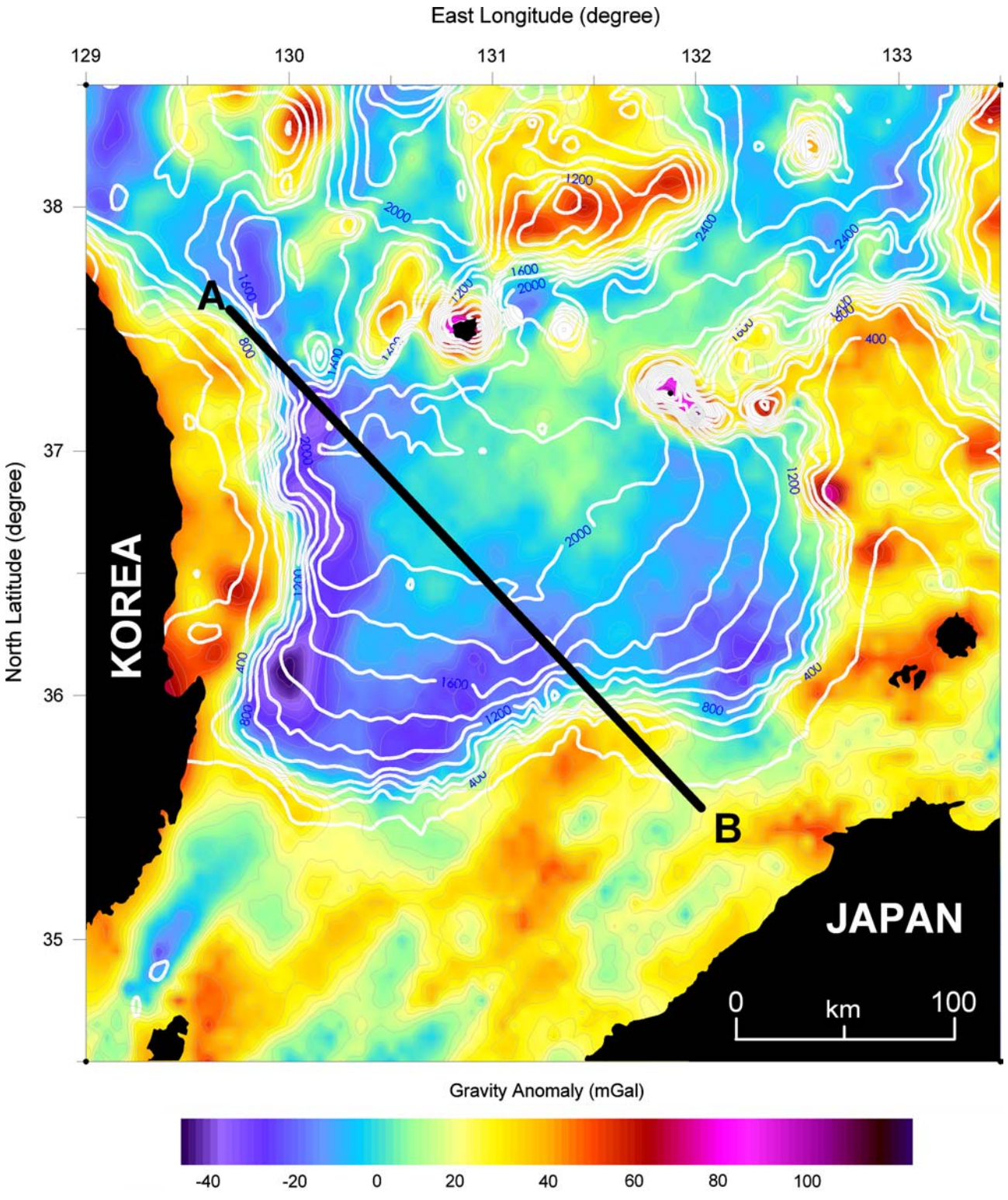

Fig. 9 Combined shipborne and satellite altimetry-derived free-air gravity anomalies from the cross-over analysis with superposed bathymetry (white contours). The gravity anomalies along profile A–B are modeled in Fig. 12

upper panel of Fig. 12, the gravity effects of these mass variations match the anomalies of Fig. 9 with negligible error along the transect.

Calculated gravity anomalies closely fit to observed anomalies for the simple basin model shown in Fig. 12 that includes continental crust overlying magmatically

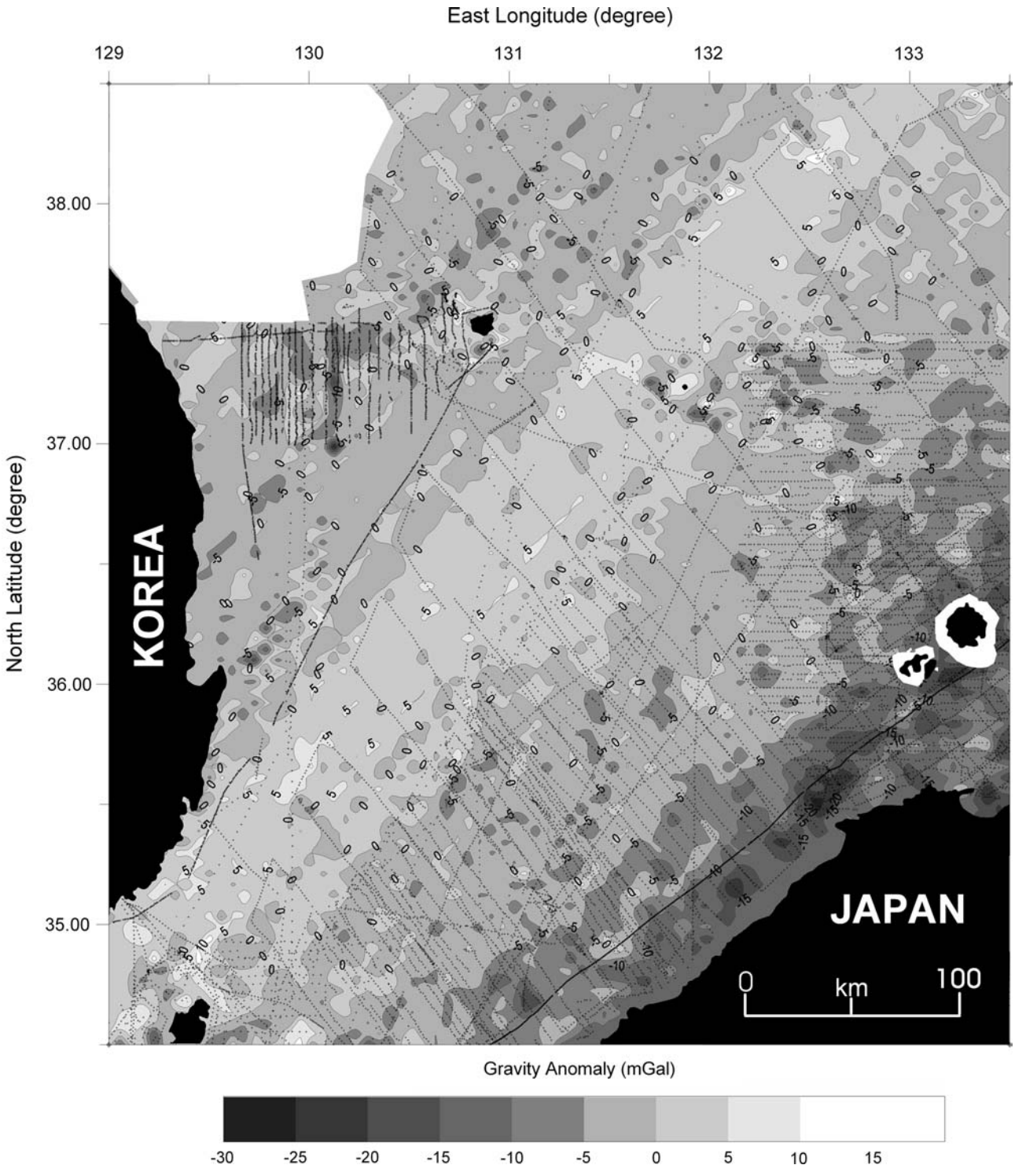

Fig. 10 Map showing the differences between the satellite altimetry-derived and the combined free-air gravity anomalies. These results were obtained by subtracting values shown in Fig. 4 from Fig. 9

underplated rocks along the margin and oceanic crust in the central part of the basin. The gravity modeling shows up to 4–5 km of sediment may overlie roughly 10 km of dense oceanic crust in the central part of the basin. Hence, the total thickness of the crust underlying the sediment may be about 14–15 km. Seismic refraction studies also indicate abnormally thick oceanic crust in the Yamato Basin (Hirata et al. 1989) and Ulleung Basin (Kim et al. 1994). Lee et al. (1999) suggested that the oceanic basement of the Ulleung

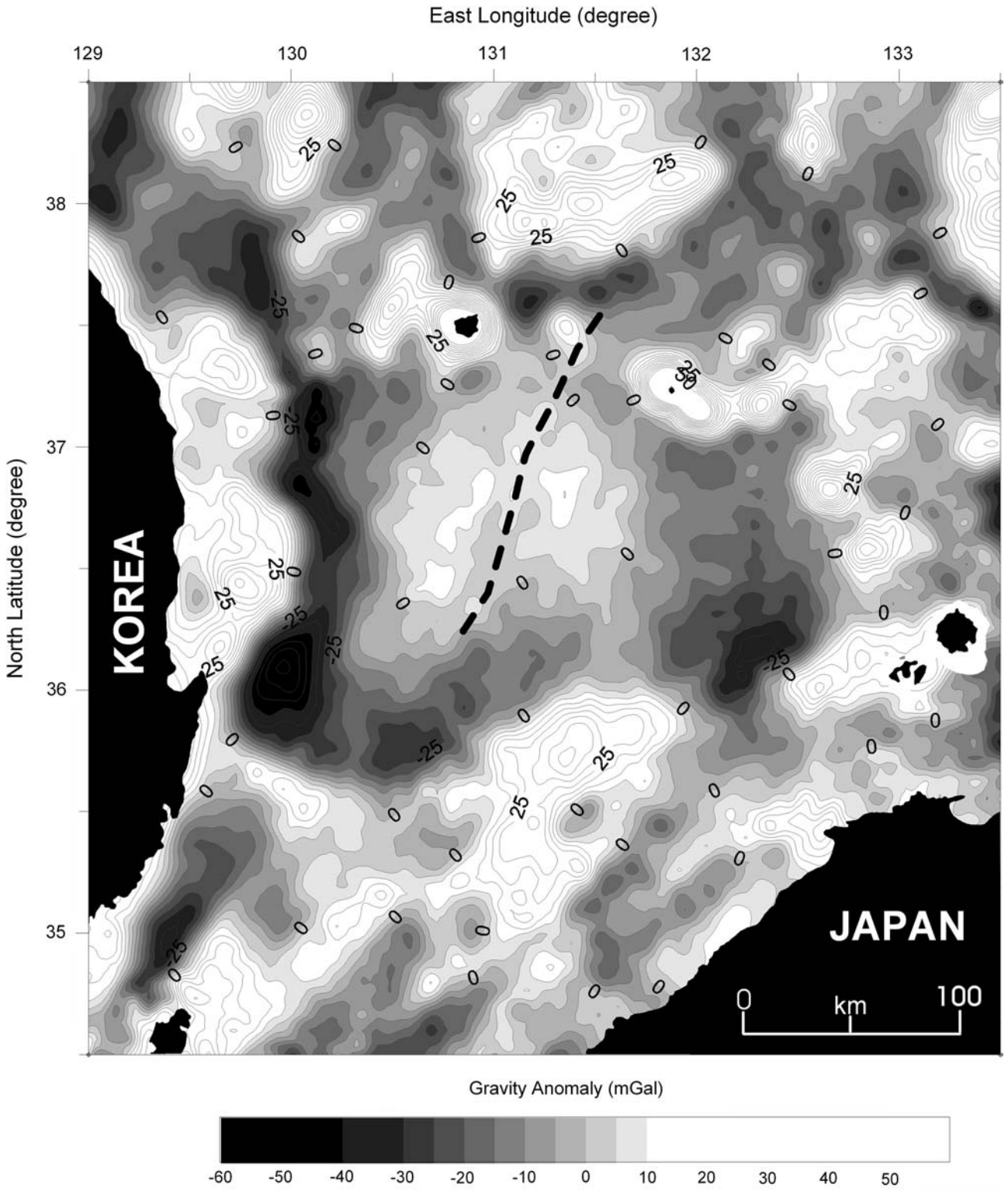

Fig. 11 Free-air gravity anomalies bandpass filtered for wavelengths between roughly 10 km and 150 km. The possible trace of the seafloor spreading ridge is delineated by the thick dashed line

Basin breaks down into two velocity layers where the lower layer is roughly twice as thick as normal oceanic layer 3. To model the crust underlying the sediments with an average seismic velocity of about 6.8 km/s (Fig. 13), we used a sediment density of 2,900 kg/m^3.

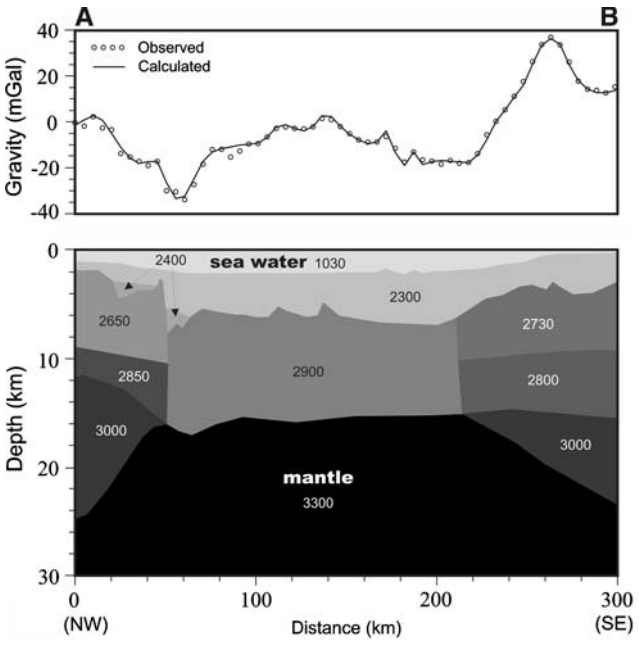

Fig. 12 Two-dimensional crustal model along transect A–B constrained by gravity (Fig. 9), bathymetry (Fig. 3) and ocean bottom seismic data (Lee et al. 1999). Location of profile is shown in Figs. 3 and 9. Numbers shown in the profile are densities given in kg/m^3

The crustal structure for the fossil spreading ridge is relatively weakly expressed, which is consistent with its poorly developed magnetic lineations (Jolivet and Tamaki 1992; Tamaki et al. 1992; Park et al. 1996) and the available bathymetric data (Fig. 3). Basin development was apparently limited to the onset of oceanic ridge and crust formation. The basin opened perpendicular to the north-northeasterly trending spreading ridge.

Care must be taken in using these results because they are not unique, as a consequence of the fundamental source ambiguity of the potential theory. Clearly, additional geophysical data, especially from magnetic and seismic surveys, can yield further insight on the crustal properties and evolution of the Ulleung Basin.

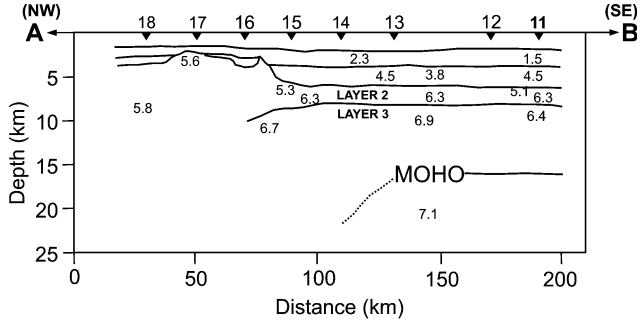

Fig. 13 *P*-wave velocities in km/s from seismic refraction data obtained in the Ulleung Basin (Lee et al. 1999). Numbered OBS locations are shown in Fig. 9

Conclusions

Cross-over analysis is useful for integrating higher frequency shipborne gravity data with more regionally consistent long wavelength satellite anomalies into an improved gravity anomaly field for geologic studies of the Ulleung Basin. The cross-over adjustments made in this study have reduced the average differences between satellite and shipborne gravity from 5.3 mGal to 0.3 mGal, and lead to a more coherent gravity map.

Gravity anomalies along the margin of the Ulleung Basin may reflect magmatic underplating, the edge effect between continental and oceanic crust, and basement topographic effects typical of passive margins. Large negative gravity anomalies at the foot of the continental slope are partly associated with sediment accumulations overlying a basement depression particularly along the western margin. The central gravity high of the Ulleung Basin overlies a deep and flat seabed and thus may reflect the enhanced mass effect of a thinned oceanic crust and shallow Moho. This oceanic crust also includes a fossil abandoned seafloor spreading ridge with about 2-km of relief from which the Ulleung Basin may have developed.

Acknowledgements We thank the geophysical group at KORDI and Prof. J.S. Won at Yonsei University for their support in collecting data. This investigation contributed to KORDI research objectives under Grants BSPE 00853-00, BSPE 00871-00 and BSPM 00203-00. Elements of this research were performed while JWK held a National Research Council Senior Research Fellowship from the NASA Goddard Space Flight Center. We thank Dr. Clift and two anonymous referees for their comments that significantly helped to improve the manuscript.

References

Blakely RJ (1995) Potential theory in gravity and magnetic applications. Cambridge University Press, 441 pp

Campbell S (1995) Southeast Asia Gravity Project, Technical Rept. GETECH (Geophys. Expl. Tech.). Dept. of Earth Sci., Univ. of Leeds, 69 pp

Celaya M, MaCabe R (1987) Kinematic model for the opening of the Japan Sea and the bending of the Japanese Islands. Geology 15:53–56

Chough SK (1983) Marine geology of Korean Seas. D. Reidel Publishing Company, Dordrecht

Chough SK, Jeong KS, Honza E (1985) Zoned facies of mass-flow deposits in the Ulleung basin, East Sea (Sea of Japan). Mar Geol 65:113–125

Hirata N, Tokuyama H, Chung TW (1989) An anomalously thick layering of the crust of the Yamato Basin, southeastern Sea of Japan: the final stage of back-arc spreading. Tectonophysics 165:303–314

Ishihara T (1984) CCOP proceedings of the 19th session, Tokyo, Japan 29 Nov.–10 Dec., Technical Report, Bankok Tailand

Jolivet L (1986) American-Eurasia plate boundary in eastern Asia and the opening of marginal basins. Earth Planet Sci Lett 81:282–288

Jolivet L, Tamaki K (1992) Neogene kinematics in the Japan Sea region and volcanic activity of the Northeast Japan arc. In: Proceedings of the Ocean Drilling Program, Science Results, 127/128(pt.2):1311–1331

Jolivet L, Hidetoshi S, Fournier M (1995) Paleomagnetic rotations and the Japan Sea Opening. In: Taylor B, Natland J (eds) Active margins and marginal basins of the Western Pacific. Am Geophys Union Geophys Monogr 88:355–369

Joshima M (1978) Gravity measurements. In: Honza E (ed) Geological investigations in the northern margin of the Okinawa Trough and the western margin of the Japan Sea. Geol Survey Japan Cruise Rept 10:21–36

Kawai N, Nakajima T, Hirook K (1971) The evolution of the island arc of Japan and the formation or granites in the Circum.-Pacific belt. J Geomag Geoelectr 23:267–293

Kim HJ, Park CH, Hong JK, Jou HT (1994) A seismic experiment in the Ulleung Basin (Tsushima Basin), southwestern Japan Sea (East Sea of Korea). Geophys Res Lett 21:1975–1978

Kimura G, Tamaki K (1986) Collision, rotation, and back-arc spreading in the region of the Okhotsk and Japan Seas. Tectonics 5(3):389–401

Knudsen P (1987) Adjustment of satellite altimeter data from cross-over differences using covariance relations for the time varying components represented by Gaussian functions. Proc IAG Symposia TOME II: 617–628

Lallemand S, Jolivet L (1985) Japan Sea: a pull-apart basin? Earth Planet Sci Lett 76:375–389

Lee GH, Kim HJ, Suh MC, Hong JK (1999) Crustal structure, volcanism, and opening mode of the Ulleung Basin, East Sea (Sea of Japan). Tectonophysics 308:503–525

Lister GS, Etheridge MA, Symonds PA (1991) Detachment models for the formation of passive continental margins. Tectonics 10:1038–1064

Oshida A (1992) Basement topography and magnetic anomalies in the Japan Sea. Ph.D. Thesis, Univ. of Tokyo, Japan

Otofuji Y, Matsuda T (1983) Paleomagnetic evidence for the clockwise rotation of southwest Japan. Earth Planet Sci Lett 62:349–359

Otofuji Y, Matsuda T, Nohda S (1985) Opening mode of the Japan Sea inferred from the paleomagenetism of the Japan arc. Nature 317:603–604

Park KS (1990) The seismic stratigraphy, structure and hydrocarbon potential of the Korea Strait. Ph.D. Thesis, Imperial College, London, 441 pp

Park SJ (1998) Stratal patterns in the southwestern margin of Ulleung Back-arc basin: a sequence stratigraphic analysis. Ph.D. Thesis, Seoul National University, Seoul, 176 pp

Park CH, Kim HJ, Yang CS, Suk BC, Isezaki N (1996) Crustal structure of the Ulleung Basin, the East Sea (Japan Sea), from gravity and ocean bottom seismometer data. J Geol Soc Korea 32:276–290

Prince RA, Forsyth DW (1988) Horizontal extent of anomalously thin crust near the Vema Fracture Zone from the three-dimensional analysis of gravity anomalies. J Geophys Res 93:8051–8061

Sandwell DT, Smith WHF (1997) Marine gravity anomalies from Geosat and ERS-1 satellite altimetry. J Geophys Res 102(B5):10,039–10,054

Sasajima S (1981) Pre-neogene Paleomagnetism of Japanese Iasands (and Vicinities). In: McEllhinny NW, Valencio DA (eds) Paleoreconstruction of the continents, Geodyn. Ser., 2, AGU, Washington, D.C. and GSA, Boulder, Colorado, pp 115–128

Suh MC, Lee MK, Suk BC (1993) Geological structure of the Ulleung Basin from marine gravity data. J Geol Soc Korea 29(2):119–127

Tamaki K, Pisciotto KA, Allan J (1990) Background, objectives, and principal results, ODP Leg 127, Japan Sea. In: Proceedings ODP, Init Repts 127:5–23

Tamaki K, Suyehiro K, Allan J, Ingle JC Jr, Pisciotto KA (1992) Tectonic synthesis and implications of Japan Sea ODP drilling. In: Proceedings ODP, Sci Results 127/128(Pt. 2):1333–1348

Torge W (1989) Gravimetry. Walter de Gruyter, New York, p 465

Wessel P (1989) Xover: A cross-over difference detector for track data. Comput Geosci 15:333–346

Wessel P, Smith WHF (1995) New version of the Generic Mapping Tools released. EOS Trans AGU, 75:329

Wessel P, Watts AB (1988) On the accuracy of marine gravity measurements. J Geophys Res 93:393–413